

# A Coupled Piezoelectric and Electromagnetic Energy Harvester with Feed forward and Feedback PWM converter for Vibrational Energy Harvesting

S. Banik

*B.E Power Engineering, Jadavpur University, Kolkata, West Bengal, India*

**Abstract-** Harvesting energy from human body motion is becoming a popular aspect of interest recently. This energy is clean and can be very useful for energizing small devices like smartphone and watches. There are many ways available for harvesting energy from low frequency vibration sources, like piezoelectric harvesters, electrical mechanical harvesters, Triboelectric generators etc. This paper provides a design of coupled electromagnetic and piezoelectric generator where a free moving mass coupled with magnets moves inside a tube to generate electrical energy by induction and also by impact at both ends simultaneously, utilizing piezoelectric material. The output energy is then fed into a power conditioning circuit which consists of a harvester circuit and PWM DC-DC boost converter circuit. Harvester output at different frequency and at various load is tested. A DC-DC Converter model is developed in SIMULINK and simulated.

**Index Terms-** Electromagnetic, Piezoelectric, Energy Harvester, Boost Converter, PWM.

## 1. INTRODUCTION

With the advancement of technology small portable utility devices like smartphone, smart watches are

Author, Year	Method	Power/Frequency	Reference
Fan, 2017	PZT	0.35 mW/0.9Hz	2
Kuang, 2016	PZT	5.8 mW/0.9 Hz	3
Wu, 2017	Electromagnetic	2.3 mW	4
Geisler, 2017	Electromagnetic	3.94 mW @ 6.4 km/h	5
Morais, 2011	Electromagnetic	6.5 mW @ 1.85 Hz	6

Table 1

becoming an integral part of our life. However running these devices require a considerable amount of energy. With limited energy storage that a conventional battery provides, additional energy sources are required to compensate for this deficiency. Even if we don't notice but a very significant amount is being lost in form of vibration almost everywhere. Human body motion is itself can be a great source for harvesting energy. At 20 kg of payload human elbow is able to produce 1.2 watt at a moment of 1.2 [N] [1], about 36.4 W is generated by knee at a moment of 40N [1]. Where the requirement of a regular smartphone battery is about 2 -6 W while charging. There has been a lot of work on generating energy from human motion using piezoelectric and electromagnetic generator individually. Table 1 provides basic description of harvesting devices and power obtained at corresponding frequencies. In [6] there is an electromagnetic generator with magnetic springs at the both side of moving slider. The power output was found to be 224  $\mu$ W at a frequency of 4.4 Hz with coil width 10 mm and tube length 56 mm. However in these systems there is a resonant frequency at which the extracted power is maximum,

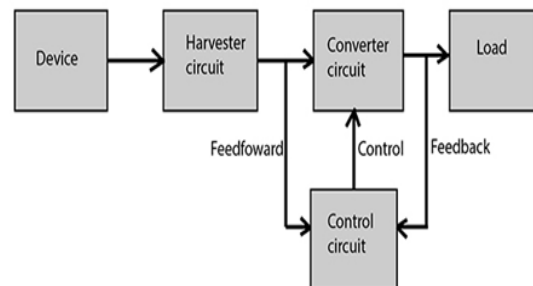


Fig 1. Block diagram of the overall system [5]. Considering the irregularity of vibrating sources, it is very difficult to tune the system to match this frequency.

In this paper an Electromagnetic generator is designed and developed with a free moving magnetic slider with piezoelectric plate attached at both sides. Along with generating electrical energy by induction when on the move, the slider generates additional electrical by impacting the piezoelectric plates at each extremes. Low frequency hand shaking movement (2-7Hz) is used for power generation. Power developed is fed to a harvester circuitry Fig 5 and power delivered to the resistive load measured. A control circuitry is developed to generate PWM based on input and output voltage level to run a DC- DC boost converter. The converter model is developed in SIMULINK and the output is presented in the experimental result section

## 2. DESIGN AND MODELLING

### 2.1. ELECTROMAGNETIC GENERATOR

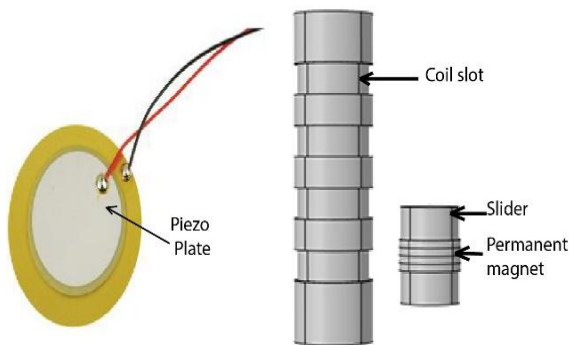


Fig. 2. Basic structure of Electromagnetic harvester Fig 4 shows the schematic diagram of Electromagnetic generator. PVC tube of length 85 mm is used with slotted section as shown. Length of each coil slot is 8mm. The coils are connected in series. The slider consists of two mild steel section and 4 NdFeB of grade N42 rare earth magnets stacked together. Holes are drilled on the mild steel section for housing balls Fig 7 (b) which will provide it rolling motion. The whole slider section works as a single magnetic pole. As the slider moves inside the tube periodically, flux associated with coils changes, inducing voltage within the coil according to faraday’s law of electromagnetic induction.

### 2.2. PIEZOELECTRIC GENERATOR

Piezoelectric materials have the ability of producing electricity when subjected to mechanical stress.

The electrical and mechanical behavior can be modeled by the two constitutive equations

$$S = s^E T + d_t E \quad (1)$$

$$D = dT + \epsilon^T E \quad (2)$$

Where  $S$  is the mechanical strain,  $T$  is the applied mechanical stress in (N/m<sup>2</sup>),  $E$  is the Electric field,  $D$  is the electric displacement in (C/m<sup>2</sup>),  $s^E$  is the matrix of elasticity in (m<sup>2</sup>/N) under conditions of Constant electrical field,  $d$  is the piezoelectric coefficient matrix (C/m<sup>2</sup> per N/m<sup>2</sup>), and  $\epsilon^T$  is the permittivity matrix in (F/m) at constant mechanical strain. This makes them very useful for small energy harvesting application. As in our design piezoelectric plate Fig 3 attached on the both side of the tube. When the slider reaches any of the extremes, it strikes the plates to generate electricity.

## 3. ANALYTICAL MODELLING

### 3.1. DYNAMIC MODELLING

Fig 3 shows a conceptual diagram of the device under working condition. The device moves like a pendulum, the motion of which is quite similar to that of our wrist movement. When the harvester reaches on one of it extremes and about to go in the reverse direction, the slider [Fig 3] is having kinetic energy of  $\frac{1}{2} M v^2$ , where  $m$  is the mass of slider, starts moving towards the opposite extremes [side B]. The equation of the motion for the slider is given as

$$F_{net} = F_{int} - Mg \sin \theta - F_{fric} - F_{ele} \quad (3)$$

Parameters	Value
Tube length (mm)	100
Inner dia (mm)	21
Outer Dia (mm)	24
Coil Resistance ( $\Omega$ )	4.4
Magnet Dia (mm)	18
Magnet Thickness (mm)	2
Coil length (mm)	9
Coil thickness (mm)	3
Slider height (mm)	25
Slider diameter (mm)	17
Number of turns in each coil	160
Number of coil	4
Dia of the piezoelectric plate (mm)	25

Table 2. Device Parameters

Where  $F_{int}$  the inertial force is generated by stipulated movement of harvester,  $Mg \sin \theta$  is the force due to gravity pulling it backward,  $F_{fric}$  is the force due to

dynamic friction and  $F_{ele}$  is the force due to electrical damping.

The total energy balance equation is given by

$$\frac{1}{2} Mv^2 = E_{fric} + Mgl \sin \theta + E_{elec,ind} + E_{elec,piezo} + E_{imp} \quad (4)$$

Where  $E_{fric}$  the energy lost due to friction is,  $Mgl \sin \theta$  is the gain in the gravitational potential energy,  $E_{elec,ind}$  is the energy generated by electromagnetic induction,  $E_{elec,piezo}$  is the energy generated from the piezoelectric plates and  $E_{imp}$  is the energy lost because of non elastic collision at the extremes.

### 3.2. MODELLING OF GENERATED VOLTAGE

From the faradays law of electromagnetism the induced emf in a coil directly proportional to the rate of change of flux linkage associated with it.

$$e = -N_c \frac{d\phi}{dt} \quad (5)$$

Where  $e$  is induced emf in the coil,  $\phi$  is flux that is linking the coil and  $N_c$  is number of turns in the coil.

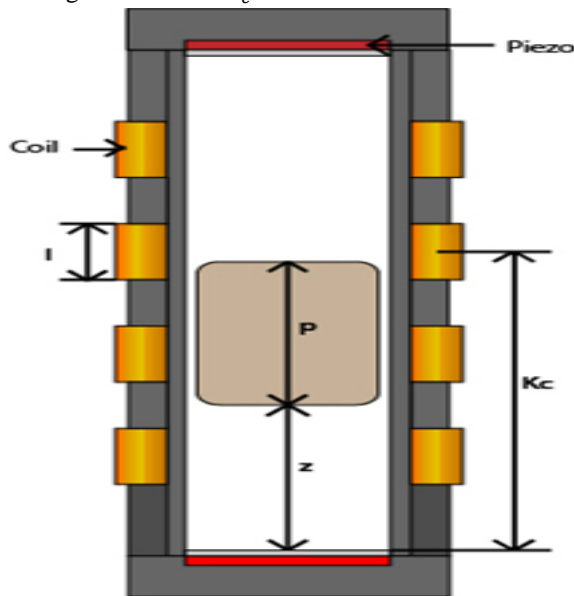


Fig 3. Basic model of the device

Fig 4(a) shows the magnetic flux density distribution along the slider. Fig 4(b) shows flux density distribution in the axial direction of the slider. The flux density distribution can be approximated as a sin curve and flux linkage to any coil whose center is residing at a height  $k_c$  is given by

$$\phi(z) = \phi_{max} \int_{k_c - \frac{1}{2}}^{k_c + \frac{1}{2}} \frac{N_c}{l} \cdot \sin\left(\frac{\pi}{p}(k - z)\right) dk \quad (6)$$

Where  $p$  effective pole distance,  $z$  is the distance between bottom of the pole and base and  $l$  is the thickness of the coil. In this case the radial variation of flux density is neglected because of the small thickness of coil. Hence the induced emf is given by

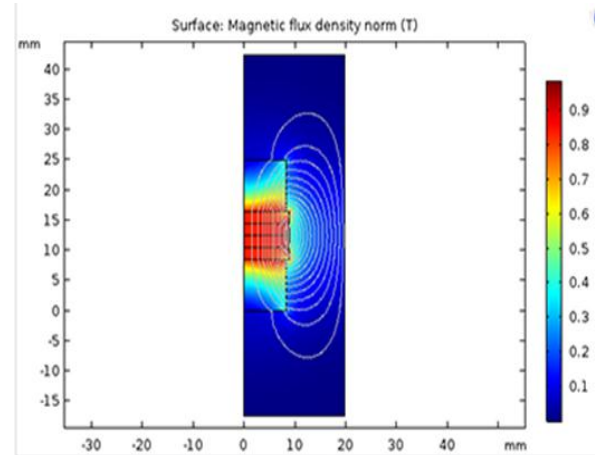
$$e(z) = -2 \frac{N_c}{l} \cos\left(\frac{\pi}{p}(k_c - z)\right) \sin\left(\frac{\pi l}{2p}\right) \frac{dz}{dt}$$

$$\text{When } k_c - p - \frac{1}{2} \leq z \leq k_c + \frac{1}{2} \quad (7)$$

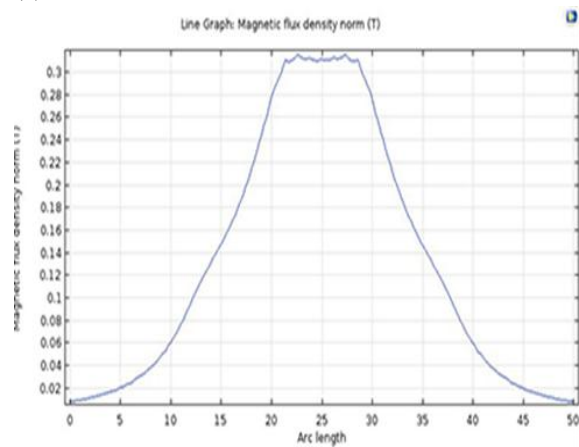
As all the coils are connected in series to determine net emf induced in the coil, we just replace the  $k_c$  in the above equation by  $k_c \pm ix$ , where  $x$  is the distance between the center of the coils and  $i = 1, 2, 3, 4 \dots$ . Hence the net equation becomes

$$e(z_i) = -2 \frac{N_c}{l} \cos\left(\frac{\pi}{p}(k_c \pm ix - z)\right) \sin\left(\frac{\pi l}{2p}\right) \frac{dz}{dt}$$

$$\text{When } k_c \pm ix - p - \frac{1}{2} \leq z \leq k_c \pm ix + \frac{1}{2} \quad (8)$$



As in our case, all the coils are connected in series, (a)



(b) Fig 4. (a) Magnetic flux density distribution along the slider (b) Flux density distribution in axial direction to find the total resultant voltage, individual voltage in

each coil is added algebraically according to the spatial position of the rotor.

4. POWER HARVESTER CIRCUIT

Fig 5 is the basic power harvester circuit that has been used as primary energy harvesting from the device. Electromagnetic harvester is connected across a full wave voltage doubler circuit. As the voltage that is generated by the piezoelectric plates upon each striking is more than that of Electromagnetic harvester, hence the piezoelectric plates are

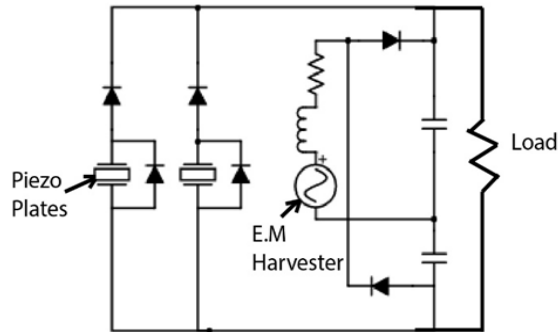


Fig 5. Harvester Circuit

Connected in parallel with the Electromagnetic harvester as shown. The diodes connected across them shorts the piezoelectric plates during their negative cycle so the charge required for the inherent capacitance to get themselves charged up to positive peak voltage becomes very less.

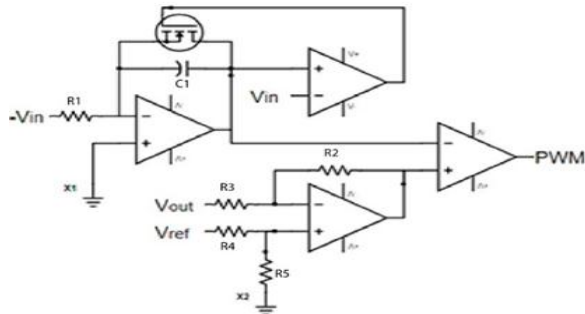
5. PROPOSED CONVERTER CIRCUIT

Proposed switching period of the converter. If L be the inductance of the inductor then

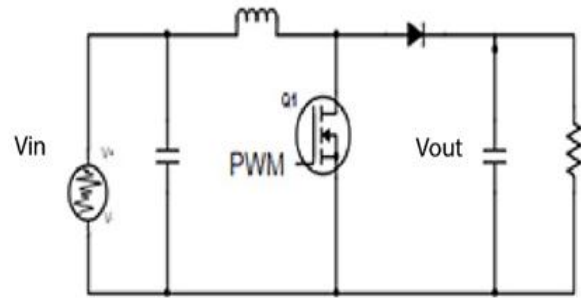
$$V_i = L \frac{di_L}{dt} \tag{9}$$

Where  $V_i$  is the voltage across the inductor and  $i_L$  is the inductor current. Now for the boost converter the output voltage  $V_o$  is given by

$$V_o = \frac{V_i}{(1-D)} \tag{10}$$



(a)



(b)

Fig 6. (a) PWM generator circuit (b) DC-DC converter

And the critical value of the inductor that is required for the converter to remain discontinuous conduction mode is given by

$$L_c = \frac{D \times V_i \times (1-D) \times T}{2I_o} \tag{11}$$

Where  $L_c$  is the critical value of resistance, and  $I_o = \frac{P_o}{V_o}$ . Where  $P_o$  is the average output power of the converter. The inductor value must be less than the critical value of the inductance.

The control circuitry is shown in the Fig 6 (a) It

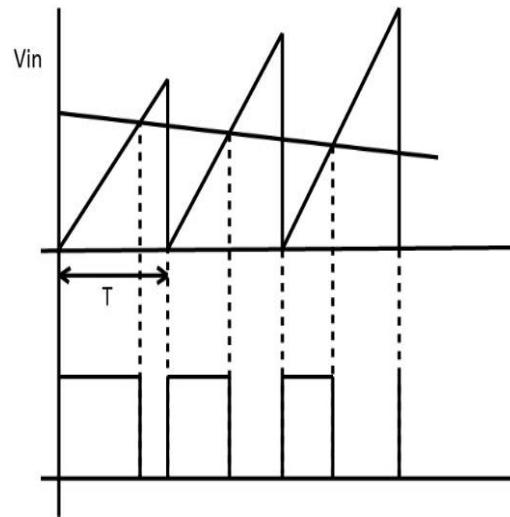


Fig 7. Generation of PWM

Consists of one integrator, one difference amplifier and two comparator. Output of one comparator is fed back to a mosfet which resets the integrator, as the output of the integrator reaches input voltage.

Let  $C_1$  be the capacitance of the integrator and  $R_1$  be the resistance of the integrator. The output voltage of the integrator is given by

$$V_s = -\frac{1}{R_1 C_1} \int_0^t V_{in} dt \quad (12)$$

Now if T be the reset time period and  $-V_{in}$  be the input of the integrator then output waveform will be a sawtooth with time period

$$T = R_1 C_1 \quad (13)$$

However the peak value of sawtooth will be proportional to the input voltage  $V_{in}$  Fig. 6 Differential amplifier compares the output voltage with the reference and amplifies the error signal. Output of the differential amplifier is given by

$$V_{diff} = \frac{R_2}{R_3} (V_{ref} - V_{out}) \quad (14)$$

Output of the differential amplifier and the integrator is compared to generate the PWM wave which drives  $Q_1$  of the converter

## 6. EXPERIMENTAL RESULT AND SIMULATION

### 6.1 HARVESTER

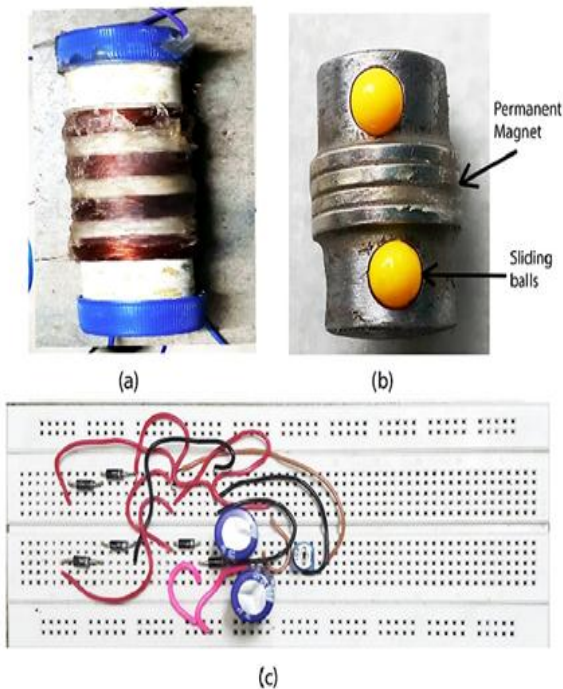


Fig. 8 (a) Complete device (b) Slider (c) Harvester circuit

The magnetic flux distribution is simulated in COMSOL multiphysics software using FEA Fig 4(a,b). For performing experiments, the device is attached on the wrist horizontally and is shaken at normal hand shaking frequency. An accelerometer is also connected with it to measure frequency and

acceleration. The power generated is fed to a resistive load via the circuit shown in Fig 5.

The flux density distribution along the pipe almost looks like a sinusoid, however there are some deformities that causes harmonics in the generated voltage Fig 9.

The generated power varies with the load resistance. At certain resistance the load power becomes maximum. Also the total power that is generated varies with frequency of the hand movement Fig.10. (d). Since frequency is directly proportional to speed, hence the generated voltage will also vary with frequency (8). However in case of normal hand vibration, frequency ranges up to 8 Hz.

For current design theoretically the frequency can be increased indefinitely but high frequency increases the impact force on the piezoelectric plates and may end up damaging them. So the frequency of vibration is kept under 7 Hz in our experiments.

The voltage waveform shown in the figure 9 is at 3.56 Hz of hand shaking frequency. The clamped voltage waveform is having a positive peak of about 0.7-0.8 V and a negative peak of 1-1.2V.

Fig 10 (a,b,c) shows the output power of the harvester at various frequency with a fixed load resistance of 250 Ohm.

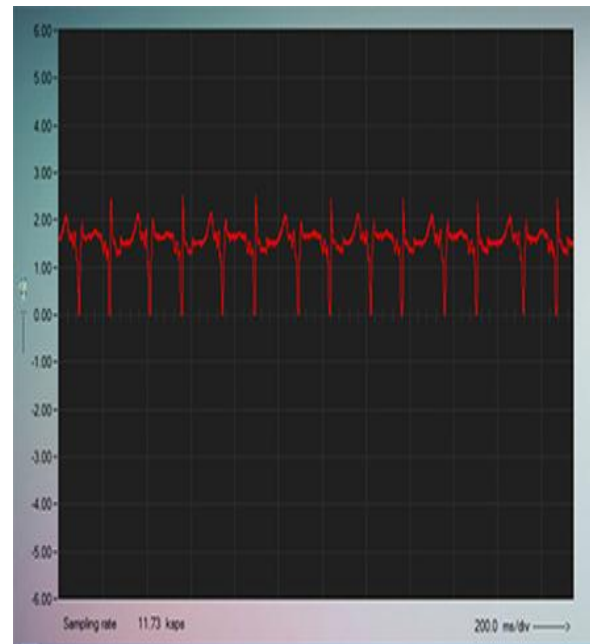


Fig 9. Generated voltage waveform of Electromagnetic harvester at 3.56 Hz

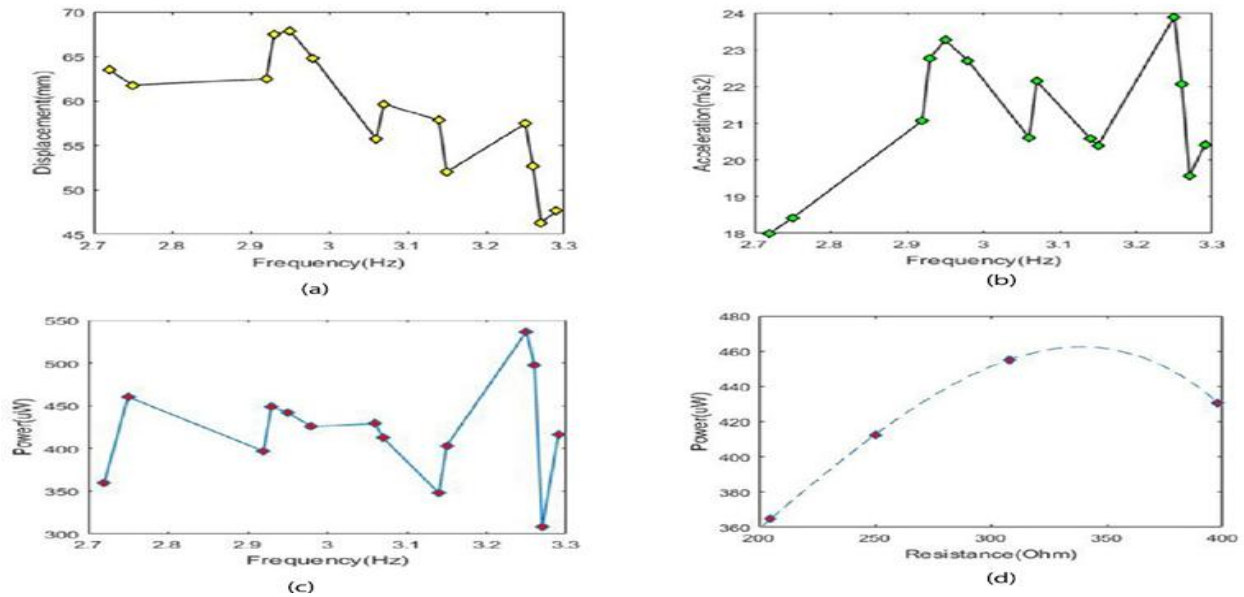


Fig 10. (a) Displacement vs Frequency (b) Acceleration vs Frequency (c) Generated power at various frequency (d) Output power at different load resistance

Fig 10 (d) shows the power output of the device at various frequency as well as their corresponding displacement and acceleration. Also d shows the variation of power output at various load resistance at 3.02 Hz. Maximum power is delivered at a load resistance of 310 ohms. When the load resistance matches the output impedance, maximum power is transferred.

It is clearly evident from the Fig 10 (a), (b), (c) is that the power generated at certain frequency is not only proportional to the acceleration at which the device is being shaken but also at the amplitude of the displacement. This is because, in case of high acceleration at small displacements the velocity that that slider will attain upon reaching at any extremes will be less hence the generated power will also be less (4). Same happens when the acceleration is less but the displacement is high.

## 6.2. CONVERTER SIMULATION

Working model of proposed converter model Fig 11 is developed and simulated in Simulink. The proposed converter works based on generation of PWM from feed forward and feedback control loops. Feedforward loops generates fixed frequency sawtooth waveform with its peak value proportional to the input voltage The sub system in Simulink Fig 12 (a) performs this task. And the feedback path compares the output voltage with the reference Fig 12 (b) and generates an error signal which is then

compared to the triangular wave to generate required PWM wave. The whole simulation model is shown in the figure. The converter was made to act in DCM mode. The operating frequency was chosen to be 1kHz, the inductor value is 150 uH, input capacitor is of 0.1uf and the output capacitor is of 0.1uf. the. From prior knowledge of the output of our device, the input voltage varies form 0-1.5V. Desired output is to be 4V.

A step voltage of 1V Is given to the system as input at 1 sec. The output voltage of the system is shown in the Fig 13 (d).

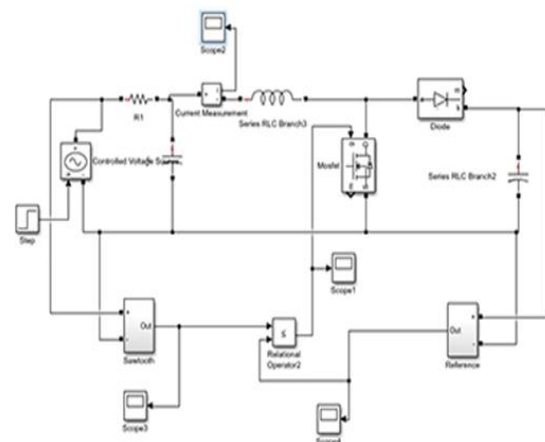
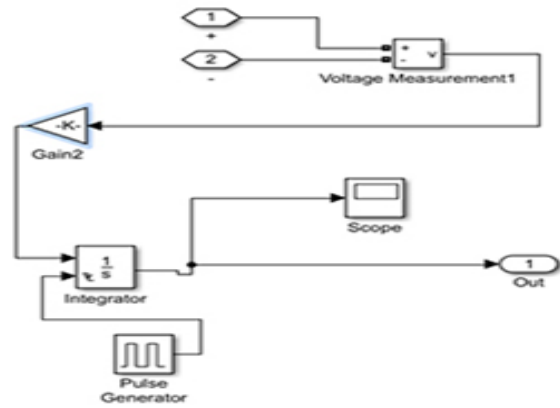
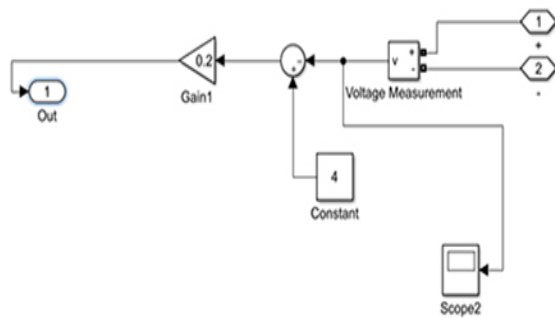


Fig 11. Simulink model of the proposed converter Fig 13 (a), (b) shows the inductor current, generated PWM wave. Inductor current is in DCM mode. Output voltage reaching the steady state within 3-4s of simulation.

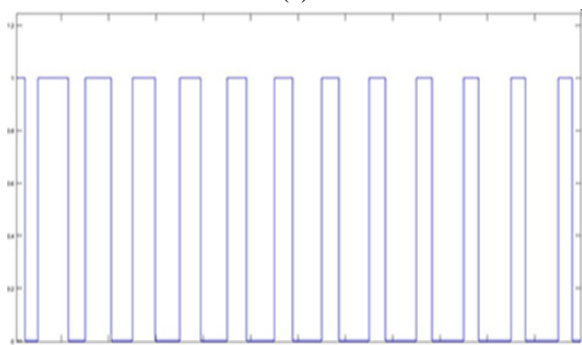


(a)

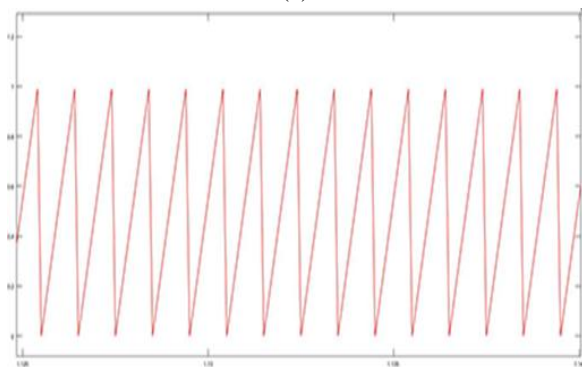


(b)

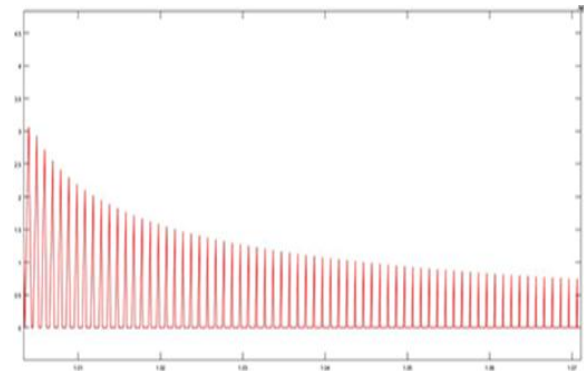
Fig 12 (a) Subsystem 1 (b) Subsystem 2



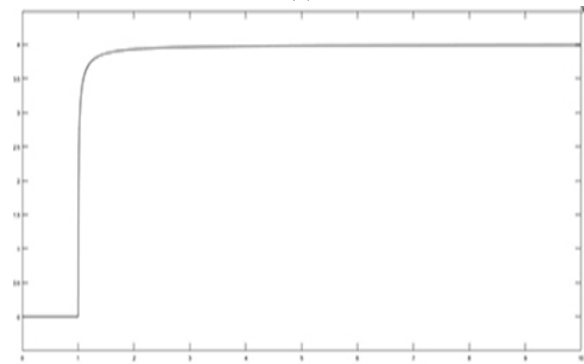
(a)



(b)



(c)



(d)

Fig 13 (a) PWM wave (b) Generated triangular wave (c) Inductor current (d) Output of the converter

## 7. CONCLUSION

Design and modelling of a coupled Electromagnetic and piezoelectric energy harvester is presented to harvest energy from low frequency (1-5Hz) vibrational sources like human body motion. Also modelling and simulation of DC-DC boost converter is presented. A control circuitry is developed and modelled which generates PWM based on feedforward and feedback of the input voltage. A working model of the device is also made and experimented at low frequency hand shaking movement. The power output at various frequency has been plotted. The maximum power output was found to be  $458 \mu\text{W}$  at a frequency of 3.23 Hz with displacement of 5.75cm and acceleration of  $24 \text{ [(m/s)}^2\text{]}$ . The output simulation of the converter shows that the voltage reaches steady state in about 2-3s after the step input is given. The design provided can be scaled down to and connected in combination to generate more power for practical application

## REFERENCE

- [1] Young-Man Choi, Moon Gu Lee, Yongho Jeon, Wearable Biomechanical energy harvesting technologies, *Energies* 2017, 10, 1483.
- [2] Fan, K. Liu, Z.; Liu, H. Wang, L. Zhu, Y. Yu, B., Scavenging energy from human walking through a shoe-mounted piezoelectric harvester. *Appl. Phys. Lett.* 2017, 110, 143902.
- [3] Kuang, Y. Yang, Z.; Zhu, M. Design and characterization of a piezoelectric knee-joint energy harvester with frequency up-conversion through magnetic plucking. *Smart Mater. Struct.* 2016, 25, 85029.
- [4] Wu, S.; Luk, P.C.K.; Li, C.; Zhao, X.; Jiao, Z.; Shang, Y. An electromagnetic wearable 3-DoF resonance human body motion energy harvester using ferrofluid as a lubricant. *Appl. Energy* 2017, 197, 364–374.
- [5] Geisler, M. Boisseau, S. Perez, M. Gasnier, P.Willemin, J. Ait-Ali, I. Perraud, S., Human-motion energy harvester for autonomous body area sensors. *Smart Mater. Struct.* 2017, 26, 35028.
- [6] Morais, R. Silva, N.M. Santos, P.M. Frias, C.M. Ferreira, J.A.F. Ramos, A.M. Simões, J.A.O. Baptista, J.M.R.; Reis, M.C., Double permanent magnet vibration power generator for smart hip prosthesis. *Sens. Actuators A Phys.* 2011, 172, 259–268.
- [7] Kangqi Fan, Jianwei Chang, Fengbo Chao, Witold Pedrycz. Design and development of a multipurpose piezoelectric energy harvester, *Energy Conversion and Management* 96 (2015) 430–439.
- [8] Shih-Wei Wang, Yi-Wen Ke, Po-Chiun Huang, Electromagnetic Energy Harvester Interface Design for Wearable Applications, *IEEE Transactions on Circuits and Systems II*, 2018.2820158.
- [9] E. Arroyo, A. Badel, Electromagnetic vibration energy harvesting device optimization by synchronous energy extraction, *Sensors and Actuators*, 171 (2011) 266– 273.
- [10] B. Lafarge, O. Curea, A. Hacala, H. Camblong, Analysis, Design & Simulation of an Electromechanical Energy Harvesting System using a Linear Movement, *First International Conference on Green Energy ICGE* 2014.
- [11] Farag S. Alargt, Ahmed S. Ashur, Mohamed A. Shrud, and Ahmad H. Kharaz, Interleaved Boost DC-DC Converter Using Delta-Sigma Modulation Suitable for Renewable Energy Applications, *International Journal of Computer and Electrical Engineering*, Vol. 6, No. 4, August 2014.
- [12] Xinping Cao, Wen-Jen Chiang, Ya-Chin King, Electromagnetic Energy Harvesting Circuit With Feedforward and Feedback DC–DC PWM Boost Converter for Vibration Power Generator System, *IEEE Transaction on power electronics*, Vol. 22, No. 2, March 2007.
- [13] Ton-Churo Huang a, Yih-Guang Leu a, Yuan-Chang Chang b, Sheng-Yun Hou b, Cheng-Chou Li, An energy harvester using self-powered feed forward converter charging approach, *Energy* 55 (2013) 769-777.
- [14] Zhenlong Xu 1, Wen Wang 1 , Jin Xie 2, Zhonggui Xu 2, Maoying Zhou 1 and Hong Yang, An Impact-Based Frequency Up-Converting Hybrid Vibration Energy Harvester for Low Frequency Application, *Energies* 2017, 10, 1761